Desalination and Water Treatment
www.deswater.com

doi: 10.5004/dwt.2017.21434

93 (2017) 152–162
October

Study on ion-exchange behavior of Cu^{2+} and Ni^{2+} with a high-efficiency resin

Jia Qian, Minqian Qiu, Zuoxiang Zeng*, Weilan Xue*

Institute of Chemical Engineering, East China University of Science and Technology, 200237 Shanghai, China,
email: qianjia0786@163.com (J. Qian), 18717858639@163.com (M. Qiu), zengzx@ecust.edu.cn (Z. Zeng), Tel. +86-021-64253081,
email: wlxue@ecust.edu.cn (W. Xue)

Received 14 March 2017; Accepted 10 September 2017

ABSTRACT

A hydrogen type 732 cation-exchange resin (732-CR) was investigated for its ion-exchange behavior with Cu^{2+} and Ni^{2+} in aqueous solutions. The ion-exchange isotherm studies show a well fit with the Langmuir model, indicating a monolayer sorption mechanism and a maximum ion-exchange capacity (q_m) of 1.736 mmol·g^{-1} for Cu^{2+} and 2.876 mmol·g^{-1} for Ni^{2+} at 308 K, respectively. The hydrated structures were proposed to explain the difference in q_m between Cu^{2+} and Ni^{2+}. The results show a two-shell six-coordinated-hydrate with eight water molecules for Cu^{2+} and an octahedral six-coordinated-hydrate with six water molecules for Ni^{2+} are the effective components for ion exchange. The thermodynamic parameters were calculated to show that the ion-exchange process is favorable, exothermic and spontaneous.

Keywords: Ion exchange; Heavy metal ion; 732 cation-exchange resin; Hydrated structure

1. Introduction

Copper (Cu) and nickel (Ni) are some of the most important base elements in the world [1]. They have a variety of industrial application areas such as chemistry, electroplating, metallurgy, coinage, catalyst, battery, agriculture, paint, petroleum refining, rubber industries, and paint manufacturing [2–4]. When released into the environment, these metals have dangerous potentials on the aquatic life and human health because of their ubiquity, recalcitrance, bioaccumulation, and toxicity [5–6]. According to Yin et al. copper and nickel are two of eight dissolved heavy metal ions with highest concentrations presented in the Yangtze Estuary in China [7]. Therefore, water pollution by the presence of heavy metal ions is becoming a crucial worldwide environmental problem and a severe public health problem and the removal of these pollutants is necessary, making it an object of constant scientific study [8–9].

Among a number of methods for removing metal pollutants from water reported by many researchers, sorption processes in solid/liquid phase, including adsorption and ion exchange, are simple, effective and attractive methods from the technological and economical point of view [10–13]. The main advantages of ion exchange over other methods, such as chemical precipitation, solvent extraction, electrochemical processes and membrane technology, are high equilibrium exchange capacity, little sludge generation, ease of operation, relatively low costs, and possibility of regeneration and reuse [14,15]. In ion exchange system, polymeric resins are usually employed. 732 cation-exchange resin (732-CR) is a crosslinked polystyrene cation-exchange resin containing sulfonic groups, which has been widely produced and used in China. Over half of this kind of resin is produced in China and its price is relatively lower among numerous commercial resins. However, information on the ion-exchange behavior of using 732-CR in hydrogen type to remove Cu^{2+} and Ni^{2+} from aqueous solutions has not been sufficiently studied. Especially the structures of metal ions on the surface of the exchanger are barely discussed by other references.

In this study, 732 strongly acidic cation-exchange resin was used as an exchanger to remove Cu^{2+} and Ni^{2+} from aqueous solutions of different initial conditions to achieve metal removal optimum conditions and the maximum ion exchange capacity. The parameters that influence ion exchange such as contact time, pH, resin dosage, initial metal ion concentration, and temperature were investi-

---

*Corresponding author.

gated. The experimental equilibrium data was analyzed by the Langmuir, Freundlich, Temkin and Dubini-Radushkevich ion-exchange isotherm models. Kinetic and thermodynamic properties and parameters were also discussed. The difference in the maximum ion-exchange capacities between Cu^{2+} and Ni^{2+} was explained by hydrated structures of metal ions. The selectivity and regeneration performance of this resin were studied.

2. Experimental

2.1. Resin and reagents

732-CR in sodium form (Shanghai Resin Factory) was used in the experiments. Its physicochemical properties and specification are listed in Table 1. $CuCl_2·2H_2O$ and $NiCl_2·6H_2O$ were purchased from Sinopharm Chemical Reagent Co. Ethylene diamine tetra acetic acid, disodium salt (EDTA), HCl (35%), and NaOH were purchased from Shanghai Lingfeng Chemical Reagent Co. Murexide was purchased from Tianjin Fuchen Chemical Reagent Co. All reagents and chemicals were analytical reagent grade; all dilutions and washings were made by deionized water.

2.2. Apparatus

A thermostatic water bath (HH-2) was used for the batch ion exchange experiments. The Brunauer-Emmett-Teller (BET) surface area and average pore diameter of resin were measured by BET method from nitrogen adsorption-desorption isotherms using a NOVA 4200e Surface Area & Pore Size apparatus. A ZEEnit 600 model Atomic Absorption Spectrometer (AAS) was used to analyze the concentration of metals in solutions.

2.3. Batch ion-exchange procedures

The resin was washed with NaOH (1 mol·L^{-1}), HCl (1 mol·L^{-1}), and deionized water to remove possible organic and inorganic impurities. Then it was converted to H^+ form by agitating with 1 mol·L^{-1} HCl for 24 h and the excess acid was removed after several washings by deionized water. The resin was dried at 338 K to a constant weight. The metal aqueous solutions of different initial concentrations (5–50 mmol·L^{-1}) were prepared by dissolving metal chloride in deionized water.

Table 1
Characteristics of 732 cation-exchange resin

Characteristics	Value
Matrix	Styrene divinylbenzene copolymer
Functional group	Sulfonic acid
Total exchange capacity	≥4.60 mmol·g^{-1} (Na^+ form)
Particle size	0.315–1.25 mm
Specific gravity	1.19–1.29
Max. operating temp	393 K
pH range	1–14 (depending on application)
Surface area[a]	443.78 m^2·g^{-1}
Pore diametre[a]	1.80 nm

[a]Measured by N_2 isotherm adsorption.

The ion-exchange behavior of Cu^{2+} and Ni^{2+} with 732-CR was studied by the batch mode. The experiments were carried out using 50 mL of Cu^{2+} and Ni^{2+} aqueous solutions of known concentration and 0.2 g of the dried H^+ form resin in stoppered conical flasks. The flasks were placed in a water bath at constant temperature with a mechanical stirrer at 150 rpm for a certain time to achieve the equilibrium. At desired time intervals, the supernatant liquid was removed and titrated by EDTA. Several parameters such as contact time, pH, initial metal ion concentration, resin amounts and temperature were changed. Each set was repeated three times and the mean values were taken for calculation.

2.4. Competitive sorption of Cu^{2+} and Ni^{2+} from aqueous solution

The H^+ form 732-CR of 0.2 g was soaked into 50 mL aqueous solutions containing Cu^{2+} (5 mmol·L^{-1}) and Ni^{2+} (5m mol·L^{-1}) with stirring at 150 rpm for 4 h at 298 K. The pH of solutions was adjusted to 2.0 and 4.0 by using diluted HNO_3 and NaOH solution. The metal ion concentrations of the solutions were analyzed by AAS.

2.5. Regeneration and reuse studies

Regeneration of the resin attached with the metal ions was performed in a batch system with 1 mol·L^{-1} HNO_3. After ion exchange process, 0.2 g of Cu^{2+}-loaded and Ni^{2+}-loaded resin were filtered, washed with deionized water and added to 50 mL HNO_3 solution at 298 K for 4 h with stirring at 150 rpm, respectively. The regenerated resin was washed, dried, and was again used in ion exchange experiments. The adsorption-desorption tests were executed for four cycles. The ion-exchange percentage for each cycle is equal to the ratio of the ion exchange amount of regenerated resin for metal ions to that of fresh 732-CR.

3. Theoretial models

3.1. Ion-exchange equilibrium

The ion-exchange amount at time t, q_t (mmol·g^{-1}) was calculated as follows:

$$q_t = \frac{(C_0 - C_t)V}{W} \tag{1}$$

where C_0 and C_t (mmol·L^{-1}) are the concentrations of metal ions in aqueous solutions at time 0 and t, respectively. V (L) is the volume of the solution and W (g) is the weight of dried resin. When equilibrium is reached: $C_e = C_t$, and $q_e = q_t$, then the equilibrium ion-exchange capacity per unit weight of resin, q_e (mmol·g^{-1}), was calculated by the mass balance relationship.

$$q_e = \frac{(C_0 - C_e)V}{W} \tag{2}$$

3.2. Ion-exchange isotherm models

Ion-exchange data are usually descried by ion-exchange isotherms, which are the relationship between equilibrium ion-exchange capacity (q_e) and equilibrium concentration (C_e) at a given temperature. The isotherm models of Langmuir, Freundlich, Temkin and Dubinin–Radushkevich (D–R) were fitted with the experimental data to describe the equilibrium ion exchange behavior.

3.2.1. Langmuir isotherm

The Langmuir model assumes homogeneous sites on the monolayer surface have equal activation energy and there is no interaction between them. Its linearized form is expressed as Eq. (3) [16]:

$$\frac{C_e}{q_e} = \frac{C_e}{q_m} + \frac{1}{q_m K_L} \tag{3}$$

where q_m (mmol·g^{-1}) is the maximum ion-exchange capacity of the exchanger and K_L (L·mmol^{-1}) is the Langmuir constant related to the affinity of binding sites.

The separation factor or the dimensionless equilibrium parameter R_L can be obtained from Langmuir equation, which is used to predict the favorability of the ion-exchange process. The separation factor is determined by the following equation [17]:

$$R_L = \frac{1}{1 + K_L C_0} \tag{4}$$

where C_0 (mmol·L^{-1}) is the highest initial concentration of metal ions. For favorable sorption, $0 < R_L < 1$; while for unfavorable sorption, $R_L > 1$. When $R_L = 1$ or 0, the sorption to be linear and irreversible, respectively.

3.2.2. Freundlich isotherm

The Freundlich model is based on the assumption that the sorption sites are distributed on heterogeneous surface with different energies. And it is not restricted to the formation of monolayers. The linearized form of Freundlich isotherm is expressed by Eq. (4) [18]:

$$\ln q_e = \frac{1}{n_F} \ln C_e + \ln K_F \tag{5}$$

where K_F is a constant related to sorption capacity and n_F is an empirical parameter relating the sorption intensity.

3.2.3. Temkin isotherm

The Temkin model considers the effects of the heat of adsorption that decreases linearly with coverage due to adsorbate/adsorbate interactions. The Temkin isotherm is used in the following linear form [19]:

$$q_e = B \ln A + B \ln C_e \tag{6}$$

where

$$B = \frac{RT}{b} \tag{7}$$

The constant B (J·mol^{-1}) is related to the heat of sorption. A (L·g^{-1}) is the equilibrium binding constant corresponding to the maximum binding energy. The ion exchange data of Cu^{2+} and Ni^{2+} removed by 732-CR can be analyzed according to Eq. (6). A plot of q_e vs. ln C_e gives the isotherm constants A and B.

3.2.4. Dubinin–Radushkevich (D–R) isotherm

The equilibrium data were also applied to the Dubinin–Radushkevich (D–R) isotherm model to determine the nature of the removal of Cu^{2+} and Ni^{2+} by 732-CR as physical or chemical [20]. The linear form of the D–R isotherm is described by the following equation [21]:

$$\ln q_e = \ln q_m - \beta \varepsilon^2 \tag{8}$$

where β (mol^2·J^{-2}) is the activity coefficient related to the sorption mean free energy and ε is the Polanyi potential, which is given by

$$\varepsilon = RT \ln(1 + 1/C_e) \tag{9}$$

where R (J·mol^{-1}·K^{-1}) is the gas constant and T (K) is temperature. The value of the mean sorption energy (E, kJ·mol^{-1}) is calculated as:

$$E = 1/\sqrt{2\beta} \tag{10}$$

The numerical value of E is used to distinguish between physical and chemical sorption. If E lies in the range of 8–16 kJ·mol^{-1}, the sorption proceeds chemically; while $E<8$ kJ·mol^{-1} indicates that the sorption process takes place physically [22,23].

3.3. Ion-exchange kinetic models

The ion-exchange kinetics describes the relationship between the amount of metal uptake and contact time, which is an important characteristic defining the efficiency of ion-exchange process. Based on the equilibrium data, the temperature of 298K and initial metal ion concentration of 0.02 mol·L^{-1} was chosen for the kinetics study. Several kinetic models including pseudo-first-order, pseudo-second-order, Elovich equation and intra-particle diffusion model were selected to evaluate the ion-exchange kinetics data as discussed below.

Pseudo-first-order model [24]: $$\ln(q_e - q_t) = \ln q_e - k_1 t \tag{11}$$

where k_1 (min^{-1}) is the equilibrium rate constant of pseudo-first-order equation.

Pseudo-second-order model [25]: $$\frac{t}{q_t} = \frac{1}{k_2 q_e^2} + \frac{t}{q_e} \tag{12}$$

where k_2 (g·mmol^{-1}·min^{-1}) is the rate constant of pseudo-second-order equation.

Elovich kinetic model [26]: $$q_t = \frac{1}{\beta_E} \ln(\alpha_E \beta_E) + \frac{1}{\beta_E} \ln t \tag{13}$$

where α_E is the initial sorption rate of the Elovich equation, and β_E is the desorption constant related to the extent of surface coverage and activation energy constant for chemisorption.

Intra-particle diffusion model [27]: $q_t = k_i t^{1/2} + I$ (14)

where k_i is the diffusion rate constant and I is a constant related to the thickness of the boundary layer.

3.4. Ion-exchange thermodynamics

The thermodynamic behavior of ion-exchange of Cu^{2+} and Ni^{2+} with 732-CR was also measured in this study. The thermodynamic parameters including the changes in the Gibbs free energy (ΔG), enthalpy (ΔH) and entropy (ΔS) were evaluated to investigate the thermodynamic feasibility and spontaneous nature of the ion-exchange process. They can be calculated using the Van't Hoff equations [28,29]:

$$\ln \frac{C_{Ae}}{C_e} = -\frac{\Delta H}{RT} + \frac{\Delta S}{R} \tag{15}$$

$$\Delta G = \Delta H - T\Delta S \tag{16}$$

where C_{Ae} and C_e (mmol·L^{-1}) are the equilibrium concentration of metal ions in the solid phase and in solution, respectively. The values of ΔH and ΔS were calculated from the slope and intercept of the Van't Hoff plots of $\ln C_{Ae}/C_e$ vs. $1/T$.

4. Results and discussion

4.1. Removal study of Cu^{2+} and Ni^{2+} by batch mode

4.1.1. Effect of contact time

The effect of contact time on the ion exchange of Cu^{2+} and Ni^{2+} with 732-CR from aqueous solution is depicted in Fig. 1. The results show that the percentage of metal ions removed increased with increasing time, and equilibrium was established in 240 min for Cu^{2+} and 180 min for Ni^{2+}. In all following experiments, the equilibrium time was maintained at 240 min, which was considered as sufficient for the removals of both metal ions by 732-CR. The ion exchange was fast initially due to the existence of greater number of resin sites available for the exchange of metal ions. Later, as the number of remaining vacant sites on the surface as well as metal ion concentration decreasing, the ion-exchange rate slowed. The curves of metal removal vs. time were single, smooth and continuously leading to saturation, suggesting the possible monolayer coverage of metal ions on the surface of the resin [30]. The results in Fig. 1 also revealed that the removal of Ni^{2+} was faster than that of Cu^{2+} and the equilibrium ion-exchange capacity of Ni^{2+} (1.120 mmol·g^{-1}) was higher than that of Cu^{2+} (1.069 mmol·g^{-1}) in this study. The maximum percent removals were 85.48 % for Cu^{2+} and 90.61 % for Ni^{2+}, respectively. Similar results were reported in the previous studies. M.H. Morcali et al. [1] used the Lewatit TP-207 resin to treat the wastewater containing Cu^{2+} and Zn^{2+}. They found the adsorption capacity reached equilibrium after 180 min for Cu^{2+} and after 120 min for Zn^{2+}.

4.1.2. Effect of initial pH

The effect of initial pH on the removal of Cu^{2+} and Ni^{2+} by 732-CR from aqueous solution was studied by varying the initial pH of metal ion solution within the range of 1.0–5.0 for Cu^{2+} and 1.0–7.0 for Ni^{2+}. Because at pH > 5.49 for Cu^{2+} and pH > 7.53 for Ni^{2+}, the metal ions get precipitated due to the formation of their hydroxyl complexes. As shown in Fig. 2, at low pH values the percent removal of Cu^{2+} and Ni^{2+} was low due to the H_3O^+ ions of higher concentration under highly acidic conditions will compete with M^{2+} to occupy the sorption sites [31]. And the repulsive force between metal ions and protons will also hinder the ion exchange process. With the initial pH rose until the optimum pH, metal removal increased. Maximum removal percentage was obtained approximately at pH 4.0 for Cu^{2+}

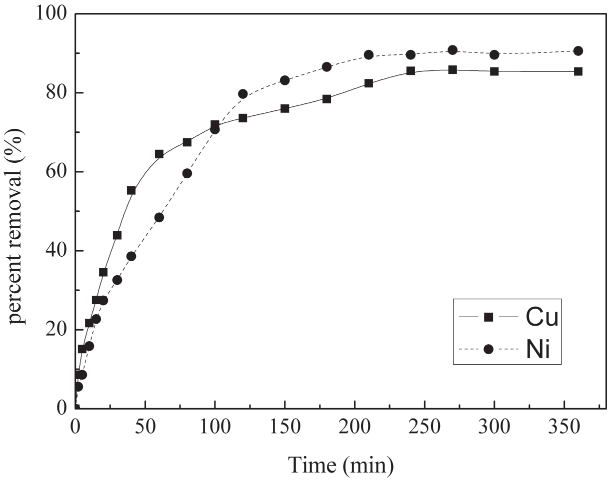

Fig. 1. Effect of contact time on removal of Cu^{2+} and Ni^{2+} by 732-CR (initial metal concentration: 5 mmol·L^{-1}; volume of metal solution: 50 mL; amount of resin: 0.2 g; pH: 4 for Cu^{2+} and 6 for Ni^{2+}; temperature: 298 K).

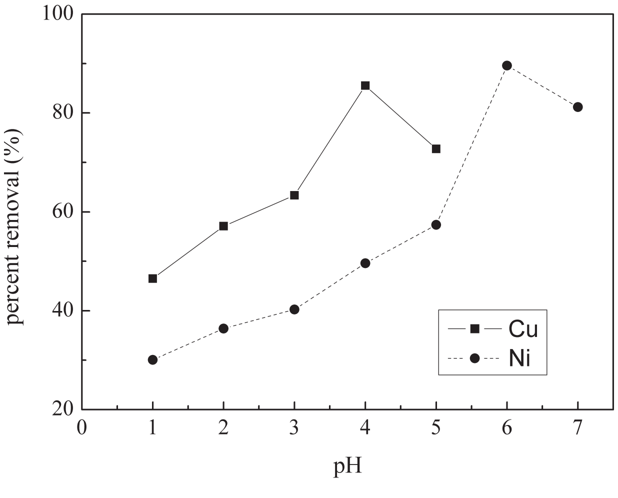

Fig. 2. Effect of initial pH on removal of Cu^{2+} and Ni^{2+} by 732-CR (initial metal concentration: 5 mmol·L^{-1}; volume of metal solution: 50 mL; amount of resin: 0.2 g; temperature: 298 K).

and 6.0 for Ni^{2+}, respectively. At pH > 4.0 for Cu^{2+} and pH > 6.0 for Ni^{2+}, the ion exchange percentage decreased slowly with initial pH increasing. One possible explanation for this decrease could be that at these higher pH values the completion of hydrolysation of metal ions in the solution phase would increasingly compete with the ion-exchange reaction [32]. Previous literature showed a similar tendency in other heavy metal ion removal studies using Lewatit TP-207 [1], Dowex [11] and Lewatit S 100 [33] sorbents with the initial pH increase. Hence, the remaining experiments were carried out at pH 4.0 for Cu^{2+} and 6.0 for Ni^{2+}, respectively.

4.1.3. Effect of resin dosage

The number of available binding sites and exchanging ions for heavy metal ions removal depending on the resin dosage used. Moreover, the resin amount is an important parameter to obtain the quantitative uptake of metal ions. Therefore, Fig. 3 shows the relationship between resin dosage and the removal of Cu^{2+} and Ni^{2+}. The amount of resin varied from 0.05 to 0.5 g at the initial metal ion concentration of 5 mmol·L^{-1}, 50 mL solution. It is apparent that the percent removal of metal ions and the removal efficiency increased with increasing resin dosage because increasing resin dose could provide a great of surface area or ion exchange sites for a fixed initial metal concentration [34]. An increase in the resin amount also resulted in a decrease in the contact time required to reach equilibrium. It can also conclude that by increasing the amount of resin, the ion-exchange density decreased. This can be attributed to the fact that some of the ion exchanger remains unsaturated during the adsorption process. When the resin dosage is bigger than 0.4 g for both metal ions, the metal ions are completely removed from the solution. It is clear from Fig. 3 that for the quantitative removal of 5 mmol·L^{-1} copper and nickel ions in 50 mL solution, a minimum resin dosage of 0.4 g is required. When the resin dosage is greater than this number, the increase in removal efficiency is negligible. Other authors also observed these phenomena when doing their researches about ion exchange or adsorption [30,34,35].

4.1.4. Effect of initial metal ion concentration and temperature

The ion exchange of Cu^{2+} and Ni^{2+} with 732-CR was studied by varying the initial metal ion concentration (5–50 mmol·L^{-1}) at three temperatures (298, 308, and 318 K). Fig. 4 shows the removal of Cu^{2+} and Ni^{2+} as a function of the initial metal ion concentration and temperature. At a certain temperature, the ion-exchange capacities for both metal ions increased with the increase of the initial concentration. A decrease in the equilibrium ion-exchange capacities for Cu^{2+} and Ni^{2+} with the increase in temperature could also be seen in Fig. 4, indicating the exothermic nature of the ion-exchange of copper or nickel ions with 732-CR. This may be due to either the damage of active binding sites in the exchanger or increasing tendency to desorb metal ions from the interface to the solution [36]. P.S. Kumar et al. [28] also found the exothermic nature of the adsorption of copper ions onto their adsorbent. However, some other authors found an increase in temperature resulted in a slight increase in the adsorption/ion exchange [2,20,29,34].

4.2. Ion-exchange isotherms

According to the plot of q_e vs. C_e at different temperatures and initial metal ion concentrations (Fig. 4) in above section, isotherm data for the ion exchange of Cu^{2+} and Ni^{2+} with 732-CR were obtained. In this study, four isotherm models (Langmuir, Freundlich, Temkin and D-R) were used to correlate the experimental equilibrium data.

The ion-exchange isotherm parameters along with the correlation coefficients (R^2) are presented in Table 2. The fitting results show that R^2 obtained from Langmuir model are very close to 1 and larger than those obtained from the Freundlich isotherms, suggesting the Langmuir model could well interpret the studied sorption procedure and the pro-

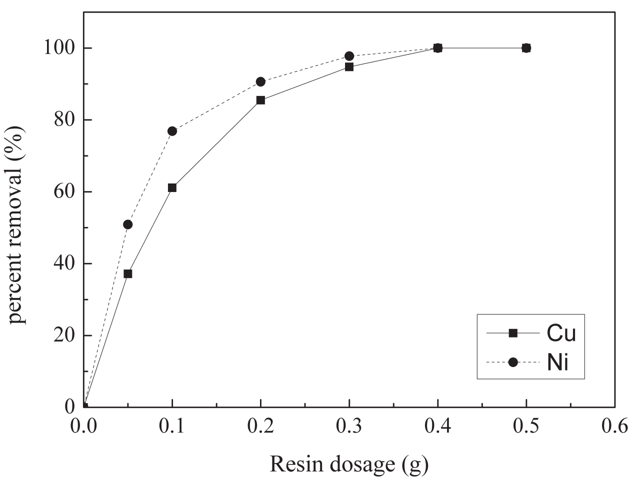

Fig. 3. Effect of resin dosage on removal of Cu^{2+} and Ni^{2+} by 732-CR (initial metal concentration: 5 mmol·L^{-1}; volume of metal solution: 50 mL; pH: 4 for Cu^{2+} and 6 for Ni^{2+}; temperature: 298 K).

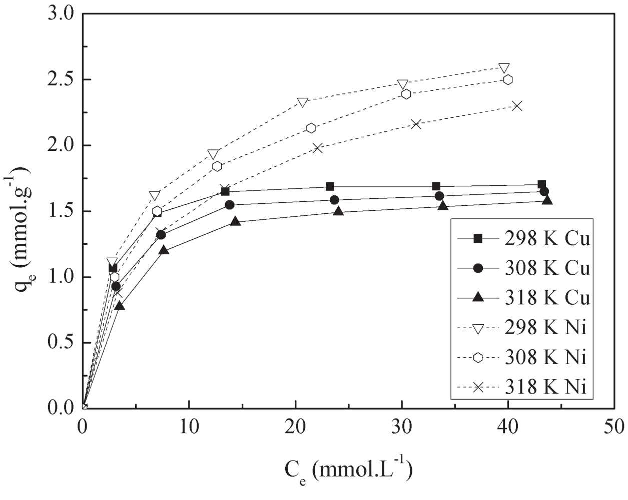

Fig. 4. Effect of initial metal ion concentration and temperature on removal of Cu^{2+} and Ni^{2+} by 732-CR (volume of metal solution: 50 mL; amount of resin: 0.2 g; pH: 4 for Cu^{2+} and 6 for Ni^{2+}).

Table 2
Ion-exchange isotherm parameters for the removal of Cu^{2+} and Ni^{2+} by 732-CR

Isotherms	Cu^{2+}			Ni^{2+}		
	298 K	308 K	318 K	298 K	308 K	318 K
Langmuir Isotherms						
q_m (mmol·g^{-1})	1.764	1.736	1.703	2.915	2.876	2.679
K_L (L·mmol^{-1})	0.720	0.432	0.286	0.192	0.154	0.137
R_L	0.0270	0.0442	0.0653	0.0946	0.1151	0.1277
R^2	0.9994	0.9994	0.9991	0.9979	0.9968	0.9982
Freundlich Isotherms						
K_F (mmol·g^{-1})	0.995	0.810	0.632	0.851	0.721	0.608
n	6.3	4.8	3.8	3.2	2.8	2.7
R^2	0.8157	0.8641	0.8750	0.9726	0.9776	0.9782
Temkin Isotherms						
B	14.09	16.75	19.26	33.20	34.32	32.98
A (L·g^{-1})	1.163	0.249	0.083	0.0451	0.0313	0.0254
R^2	0.8455	0.8995	0.9237	0.9956	0.9986	0.9996
D-R Isotherms						
q_m (mmol·g^{-1})	2.174	2.216	2.286	3.868	3.872	3.661
E (kJ·mol^{-1})	12.84	11.67	10.63	9.34	9.11	9.07
R^2	0.8786	0.9169	0.9240	0.9950	0.9961	0.9963

cess is that of monolayer sorption, rather than multilayer sorption. This may be attributed to the homogeneous distribution of sulfonic groups on the surface. From the Langmuir isotherm, the maximum monolayer ion-exchange capacities (q_m) of 732-CR are 1.736 mmol·g^{-1} for Cu^{2+} and 2.876 mmol·g^{-1} for Ni^{2+} at 308 K, respectively. Because R_L is used to predict the favorability of the sorption process, the fact that $0<R_L<1$indicates that it is a favorable process. As shown in D-R model, in the temperature range of 298–318 K, the E values of both Cu^{2+} and Ni^{2+} are higher (9.07–12.84 kJ·mol^{-1}) than 8 kJ·mol^{-1}, indicating that the ion-exchange process of Cu^{2+} and Ni^{2+} with 732-CR in aqueous solution is carried out by chemical interaction. The results also reveal it need more energy to transfer Cu^{2+} onto 732-CR than Ni^{2+}.

Table 3 lists a comparison of maximum removal capacities of Cu^{2+} and Ni^{2+} on various resins. The maximum monolayer ion-exchange capacity of 732-CR is higher than most commercial resins presented in Table 3. Therefore, 732-CR could be considered a high-efficiency material for the removal of Cu^{2+} and Ni^{2+} from aqueous solutions.

Table 3
The maximum removal capacities of Cu^{2+} and Ni^{2+} by various resins

Resins, q_m (mmol/g)	Cu^{2+}	Ni^{2+}	References
732-CR	1.736	2.876	This study
Lewatit TP-207	1.070	–	[1]
Amberjet 1200 H	0.418	–	[3]
Amberlite IRN97H	0.676		
Dowex HCR S/S	–	2.662	[8]
Dowex HCR-S	–	1.603	[11]
Amberjet 1500H	0.384	–	[12]
Ambersep 252H	0.183		
Amberlite IRC 748	1.10	–	[13]
Amberlite IR 120	1.672	–	[15]
Chelex 100	0.88	2.15	[13], [32]
Dowex 50W	2.30	2.35	[35]

4.3. Ion-exchange kinetics

Table 4 summarizes the parameters of the four kinetic models for the ion exchange process for Cu^{2+} and Ni^{2+} with 732-CR. From R^2 of various kinetics models, pseudo-second-order model is more suitable to describe the ion exchange kinetics behaviors than pseudo-first-order model. It indicates that chemisorption is the rate controlling mechanism in sorption process. This result is in accordance with the conclusion of monolayer chemical sorption of metal ions onto the resin drawn from above isotherm analysis. The Elovich model was commonly suitable to describe the adsorption kinetics of ion exchange process. The high values of the correlation coefficients of Elovich equation reveal that the sorption behaviors of copper and nickel ions on 732-CR are not only chemisorptions, but ion exchange reactions [37].

On the other hand, the values of R^2 fitted by intra-particle diffusion model are not very high. According to Eq. (14), if the plot of q_t vs. $t^{1/2}$ gives a straight line, the sorption process is controlled by intra-particle diffusion only. However, if the data present a multi-linear plot, then two or more steps influence the sorption process [38]. Base on the relatively low correlation coefficients and straight lines in the plots of q_t vs. $t^{1/2}$ in this study do not pass through the origin, it might be concluded that the intra-particle diffusion is not the only

Table 4
Ion-exchange kinetic parameters for the removal of Cu^{2+} and Ni^{2+} by 732-CR

Kinetic models	Parameters	Cu^{2+}	Ni^{2+}
Pseudo-first-order model	k_1 (min^{-1})	0.0129	0.0219
	q_e ($mmol\cdot g^{-1}$)	0.721	1.150
	R^2	0.9529	0.9887
Pseudo-second-order model	k_2 ($g\cdot mmol^{-1}\cdot min^{-1}$)	0.0257	0.0180
	q_e ($mmol\cdot g^{-1}$)	1.187	1.358
	R^2	0.9974	0.9919
Elovich model	α	0.116	0.066
	β	4.570	3.268
	R^2	0.9775	0.9807
Intra-particle diffusion model	k_i ($g\cdot mmol^{-1}\cdot min^{-1/2}$)	0.0582	0.0733
	I ($mmol\cdot g^{-1}$)	0.240	0.167
	R^2	0.8835	0.9227

rate-limiting step and both film diffusion and intra-particle diffusion may play important role in the sorption kinetics.

4.4. Hydrated structures of metal ions

Maximum monolayer ion exchange capacities (q_m) for Cu^{2+} and Ni^{2+} have been studied and the order is $Ni^{2+} > Cu^{2+}$. According to Kossel [39] and Pauling [40] the attraction between cations and anions in ionic crystals obey Coulomb's law on demands for ions of equal charge, a small ion will be attracted either to a greater force or held more tightly than a larger ion. Therefore, the ion exchange capacity should increase with decreasing ionic radii and increase with charge of ion. The ions with smaller hydrated radii easily enter the pores of sorbents, resulting in higher sorption [41,42]. The ionic radii of Cu^{2+} and Ni^{2+} are almost the same (0.72 Å) [43], while there is considerable difference in their q_m values (1.736 $mmol\cdot g^{-1}$ for Cu^{2+} and 2.876 $mmol\cdot g^{-1}$ for Ni^{2+} at 308 K), which indicates that the metal ions move inside the resin phase in the hydrated form, rather than metal ion itself. Agrawal et al. [44] drew a conclusion that during a process of metal ions adsorbed on resin beads, the ions shed most of their water of hydration at the surface of the resin and entered into the cavity in the unhydrated form where they are hydrated again and migrate towards the adsorptive sites. Since no one has investigated the hydrated structures of metal ions in the process of ion exchange with 732-CR, this study will make a discussion on this problem by combining the experimental results and theoretical analysis.

If the chemisorption process can occur on any part of the 732-CR surface without considering the effect of temperature and initial metal ion concentration, the saturated chemisorption capacity limit (q_s) can be calculated as [45]:

$$q_s = \frac{S}{A_c N_a} MW \tag{17}$$

where S ($m^2\cdot g^{-1}$) is the BET surface area of 732-CR, A_c ($Å^2$) is the surface area occupied by one hydrated structure of metal ion, N_a is Avogadro's number, and MW ($g\cdot mol^{-1}$) is the molecular weight of the hydrated structure. When q_s is taken as q_m, the A_c values of hydrated structures of Cu^{2+} and Ni^{2+} are obtained.

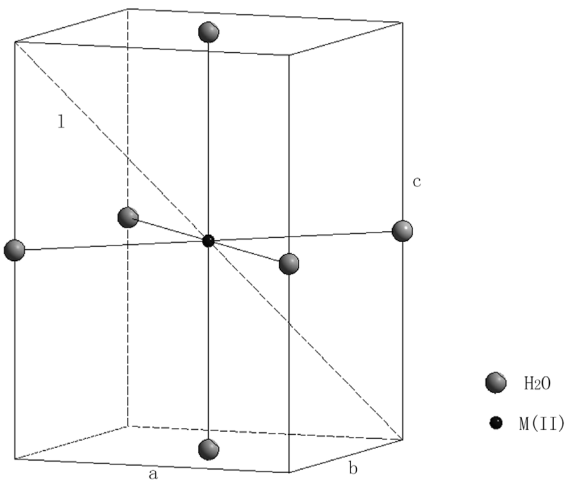

Fig. 5. Rough stereochemical structure of one hydrated metal ion complex. (Taking a six-coordinated octahedron hydrated structure for example.)

For the sake of the convenient calculation, the structure of hydrated metal cell can be simplified to a cuboid whose three sides are the cell parameters (a, b, and c), as shown in Fig. 5. Taking into consideration the space between two hydrated metal cells adsorbed on the resin surface, A_c is assumed to be the area of a square with side length l, where

$$l = \sqrt{a^2 + b^2 + c^2} \tag{18}$$

$$A_c = l^2 \tag{19}$$

The hydrate structures of Cu^{2+} are controversial [46]: Ebitani et al. [47] reported the Cu^{2+} cations displayed Jahn-Teller distorted six-coordinated octahedron with four short Cu–O distances (1.91 Å) and two long Cu–O distances (2.28 Å) in the pores of Zeolite-X by curve-fitting analysis of copper extended X-ray absorption fine structure (EXAFS) spectra. An analogous $[Cu(H_2O)_6]^{2+}$ structure has also been found in the interlayer space of montmorillonites [48]. However, Stace et al. [49] reported that the complex $[Cu(H_2O)_4]^{2+}$ and $[Cu(H_2O)_8]^{2+}$ appear to be more stable than the accepted unit $[Cu(H_2O)_6]^{2+}$, and this pattern of behavior could be attributed to a Jahn-Teller distortion of the complex.

As to the hydrate structure of Ni^{2+}, Liu et al. [50] drew a conclusion that the first coordination shell consists of six water molecules with a Ni–O coordination distance of 2.04 Å and is almost unaffected by the water molecules in the solution by density functional theory (DFT) calculations and EXAFS spectra. The similar results were also concluded by Xia et al. [51] that the first solvation shell of Ni^{2+} is an octahedral structure with six water molecules tightly bound in the $NiCl_2$ aqueous solution.

According to the above references, A_c and l values of hydrated metal clusters $[M(H_2O)_n]^{2+}$ (M = Cu or Ni, n = 4, 6, 8) are calculated using Eq. (11) and are shown in Table 5.

Table 5
Calculation results for complex $[Cu(H_2O)_n]^{2+}$ (n = 4, 6, 8) and $[Ni(H_2O)_n]^{2+}$ (n = 4, 6, 8)

Hydrated metal ion cluster	q_s (g·g^{-1})	n	A_c (Å^2)	l (Å)
$[Cu(H_2O)_n]^{2+}$	0.1103	4	89.14	9.44
		6	112.81	10.06
		8	136.49	11.68
$[Ni(H_2O)_n]^{2+}$	0.1688	4	57.08	7.56
		6	72.80	8.53
		8	88.52	9.41

Meanwhile, assumptions and calculation are carried out for the hydrated structures of Cu^{2+} and Ni^{2+} with 4 or 6 or 8 water molecules. Among them, tetrahedron and planar quadrilateral are assumed for the hydrated structures of metal ion with 4 water molecules; stretch octahedron for Cu^{2+} and octahedron for Ni^{2+} are assumed for the hydrated structures with 6 water molecules; and a two-shell structure is assumed for the hydrated structures with 8 water molecules, consisting of the six-coordinated-octahedron as first shell and remaining two water molecules as second shell. Then, taking the M–O distances from ref. [47] and [50] and the H–O distance in water molecules from ref. [52], the cell parameters (a, b, and c) for complexes $[Cu(H_2O)_n]^{2+}$ and $[Ni(H_2O)_n]^{2+}$ (n = 4, 6, 8) are obtained. Then according to Eq. (12) and Eq. (13) the cell diagonal line (l) and its surface area occupied by one hydrated metal ion cluster (A_c) are also obtained.

The results show that one of the assumed hydrated structures of Cu^{2+} and Ni^{2+} in accord with the data in table 5, respectively. That is, the hydration structure for Cu^{2+} adsorbed on the surface of the resin is a two-shell six-coordinated-hydrate with eight water molecules ($[Cu(H_2O)_8]^{2+}$). Six water molecules construct the distorted octahedron as first hydration shell whereas the seventh and eighth water molecules are in the second shell. And the hydration structure for Ni^{2+} is a six-coordinated-hydrate octahedron with six water molecules ($[Ni(H_2O)_6]^{2+}$). Their hydrated structures are shown in Fig. 6 and their cell parameters are listed in Table 6.

The results of the hydrated structures and cell parameters can be used to explain the phenomena that faster removal of Ni^{2+} from aqueous solution than Cu^{2+}, higher equilibrium ion-exchange capacity of Ni^{2+} than Cu^{2+}, and more energy needed to transfer Cu^{2+} into resin than Ni^{2+} in preceding part of this study.

Table 6
Cell parameters of the simplified cuboid structures for $[Cu(H_2O)_8]^{2+}$ and $[Ni(H_2O)_6]^{2+}$

Hydrated metal ion cluster	a (Å)	b (Å)	c (Å)	l (Å)	A_c (Å^2)
$[Cu(H_2O)_8]^{2+}$	8.60	4.06	6.48	11.50	132.34
$[Ni(H_2O)_6]^{2+}$	4.24	4.24	6.00	8.49	72.00

4.5. Ion-exchange thermodynamics

Experiments were conducted at 298, 308, and 318 K to evaluate the ion-exchange thermodynamic parameters. From the Van't Hoff equation, the results for the thermodynamic parameters are listed in Table 7. The values of ΔG are negative which confirms that the removal of Cu^{2+} and Ni^{2+} by 732-CR was spontaneous and thermodynamically favorable. The values of ΔH are negative which indicates that the ion-exchange process was exothermic in nature. This result is consistent with the above-mentioned case wherein the ion-exchange capacities decrease with the increasing of temperature. The positive values of ΔS result from the increased disorder at the solid/liquid interface due to the chemisorption process [53].

4.6. Competitive sorption of Cu^{2+} and Ni^{2+} from aqueous solution

The competitive sorption behavior of 732-CR was studied in a binary system containing both Cu^{2+} and Ni^{2+}, and the results are shown in Fig. 7. It was found that the ion exchange capacities were 0.500 mmol·g^{-1} for Cu^{2+} and 0.129 mmol·g^{-1} for Ni^{2+} at pH 2.0, and 0.712 mmol·g^{-1} for Cu^{2+} and 0.185 mmol·g^{-1} for Ni^{2+} at pH 4.0 under competitive condition. These values were lower than those in single solutions (Fig. 2), indicating a competition between Cu^{2+} and Ni^{2+} for the same available sorption sites, and that strong competitive sorption from the two metal ions at the same time inhibited the sorption of individual ion. The similar results were observed in the adsorption of Cu^{2+} and Ni^{2+} from aqueous solution by arabinoxylan hydrogel [6].

Fig. 7 also shows that at pH 2.0 and 4.0, Cu^{2+} was favorably removed by 732-CR over Ni^{2+} in both single and competitive sorption, and the difference between the ion exchange capacities of Cu^{2+} and Ni^{2+} in competitive sorption system was greater than that of single sorption system. This may indicates that it will be possible to selective recover

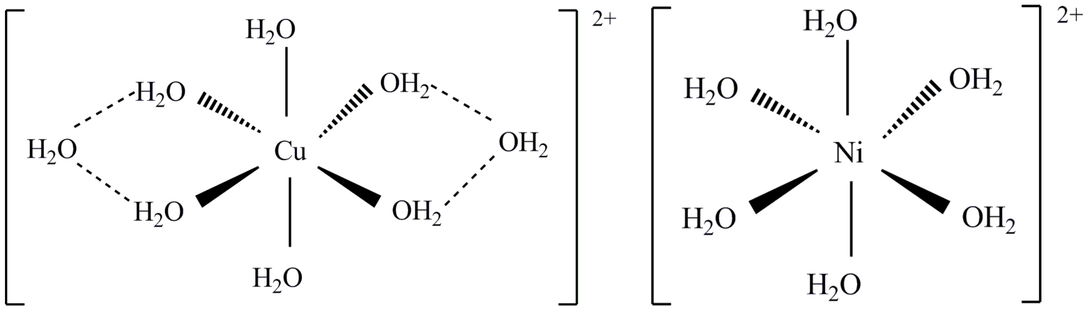

Fig. 6. Structures of hydrated metal ion complexes for $[Cu(H_2O)_8]^{2+}$ and $[Ni(H_2O)_6]^{2+}$.

Table 7
Thermodynamic parameters for the removal of Cu^{2+} and Ni^{2+} by 732-CR

Migrating ions	C_0 (mmol·L^{-1})	ΔG (kJ·mol^{-1})			ΔH	ΔS
		298 K	308 K	318 K	(kJ·mol^{-1})	(J·mol^{-1}·K^{-1})
Cu^{2+}	10	–13.78	–13.86	–13.93	–11.52	7.60
	20	–12.47	–12.60	–12.73	–8.57	13.08
	30	–11.15	–11.32	–11.49	–6.10	16.93
	40	–10.27	–10.46	–10.66	–4.46	19.49
	50	–9.66	–9.86	–10.05	–3.80	19.67
Ni^{2+}	10	–14.14	–14.25	–14.37	–10.85	11.07
	20	–13.11	–13.25	–13.38	–9.13	13.35
	30	–12.17	–12.31	–12.46	–7.81	14.60
	40	–11.49	–11.65	–11.81	–6.77	15.83
	50	–10.92	–11.09	–11.25	–6.00	16.53

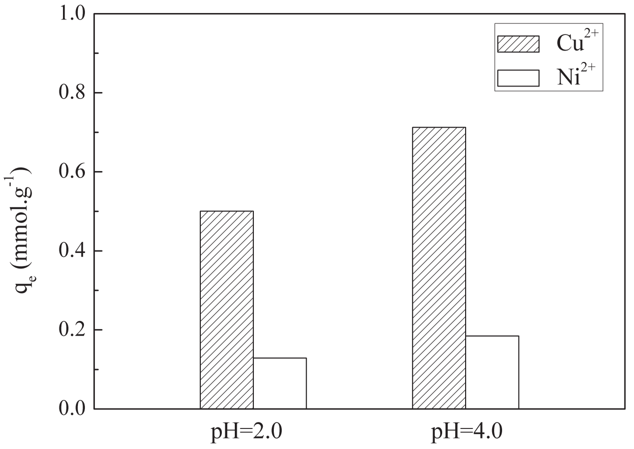

Fig. 7. Competitive sorption of Cu^{2+} and Ni^{2+} on 732-CR at pH 2.0 and 4.0.

Cu^{2+} from the binary mixture (Cu^{2+}/Ni^{2+}) at appropriate pH and other operation conditions.

4.7. Regeneration and reusability studies

In order to make the ion exchange process more economical, it is important to regenerate and reuse the exchanger. Cu^{2+}-loaded and Ni^{2+}-loaded 732-CR were treated with HNO_3 solution (0.01 M) for desorption and reused in the metal ion solutions (0.02 M) as described in the experimental part. The results of recycling behavior of 732-CR are reported in Table 8. It shows that the ion exchange capacities of Cu^{2+} and Ni^{2+} were 1.576 and 1.804 mmol·g^{-1} in the first circle, and decreased to 1.175 and 1.276 mmol·g^{-1} after four cycles, indicating that perhaps certain ion exchange sites or functional groups are decomposed or destroyed by nitric acid and hence it is expected that metal ions are weakly adsorbed in subsequent cycles [4]. 71.4% and 65.8% of sorption percentages for Cu^{2+} and Ni^{2+} could be achieved up to fourth regeneration cycle, respectively.

5. Conclusion

The batch experiments presented in this study revealed that the 732 strongly acidic cation exchange resin could be effectively used as adsorbent for removal heavy metals. For the efficient use of such an ion-exchanger, various parameters such as contact time, pH, initial metal ion concentration, resin amounts and temperature were designed to obtain the highest possible removal for metal ions. The ion-exchange isotherm analysis proved the homogeneity of resin surface and a monolayer chemical sorption mechanism. The results of kinetic study showed that the pseudo-second-order kinetic model mechanism played a significant role and there's a multi-diffusion steps controlled mechanism in the ion exchange of Cu^{2+} and Ni^{2+} with 732-CR. The maximum monolayer ion-exchange capacities (q_m) of 732-CR were 1.736 mmol·g^{-1} and 2.876 mmol·g^{-1} for Cu^{2+} and Ni^{2+} at 308 K, respectively. The hydrated structures for Cu^{2+} and Ni^{2+} were proposed to explain the difference in q_m between Cu^{2+} and Ni^{2+}. A two-shell six-coordinated-hydrate with eight water molecules for Cu^{2+} ($[Cu(H_2O)_8]^{2+}$) and a octahedral six-coordinated-hydrate with six water molecules for Ni^{2+} ($[Ni(H_2O)_6]^{2+}$) are the preferred structures for ion exchange. The thermo-

Table 8
Regeneration and reusability behaviors of 732-CR

Metal ions	Cycle 1		Cycle 2		Cycle 3		Cycle 4	
	q_e (mmol·g^{-1})	P[a] (%)	q_e (mmol·g^{-1})	P (%)	q_e (mmol·g^{-1})	P (%)	q_e (mmol·g^{-1})	P (%)
Cu^{2+}	1.576	95.7	1.494	90.8	1.311	79.6	1.175	71.4
Ni^{2+}	1.804	93.0	1.667	85.9	1.455	75.0	1.276	65.8

[a] Represents the sorption percentage, the ratio of the ion exchange amount of regenerated resin to that of fresh 732-CR.

dynamic parameters were calculated. The negative values of ΔG and ΔH revealed the spontaneous and exothermic nature of removal of Cu^{2+} and Ni^{2+} by 732-CR. And the positive values of ΔS suggested the increased randomness at the solid/solution interface. Cu^{2+} was favorably removed by 732-CR over Ni^{2+} under the competitive condition at pH 2.0 and 4.0. The regeneration of 732-CR can be made to some extent with dilute HNO_3 solution and the ion exchange capacities reduced to 71.4 % and 65.8 % for Cu^{2+} and Ni^{2+} after four cycles, respectively.

Symbols

a, b, c — Cell parameters of simplified cuboid cell (Å)
A — Constant in Temkin isotherm model
B — Constant in Temkin isotherm model
A_c — Surface area occupied by one hydrated structure of metal ion (Å^2)
C_{Ae} — Equilibrium concentration of metal ions in solid phase (mmol·L^{-1})
C_0 — Initial concentration of metal ions in solution (mmol·L^{-1})
C_e — Equilibrium concentration of metal ions in solution (mmol·L^{-1})
C_t — Concentration of the metal ion at time t in solution (mmol·L^{-1})
E — Mean free energy (kJ·mol^{-1})
I — Constant in intra-particle diffusion kinetic model (mmol·g^{-1})
k_1 — Rate constant of pseudo-first-order equation (min^{-1})
k_2 — Rate constant of pseudo-second-order equation (g·mmol^{-1}·min^{-1})
K_i — Diffusion rate constant in intra-particle diffusion kinetic model (g·mmol^{-1}·min$^{-1/2}$)
K_L — Langmuir constant (L·mmol^{-1})
K_F — Freundlich constants (mmol·g^{-1})
l — Diagonal line of simplified cuboid cell, side length of A_c (Å)
n — Coordination number
n_F — Freundlich adsorption isotherm constant
N_a — Avogadro's number
MW — Molecular weight of one hydrated structure (g·mol^{-1})
q_m — Maximum ion-exchange capacity per unit weight of exchanger (mmol·g^{-1})
q_e — Equilibrium ion-exchange capacity per unit weight of exchanger (mmol·g^{-1})
q_s — Saturated chemisorption capacity limit (mmol·g^{-1})
q_t — Ion-exchange amount per unit weight of exchanger at time t(mmol·g^{-1})
R_L — Separation fator
S — BET surface area of 732-CR (m^2·g^{-1})
T — Absolute temperature (K)
V — Volume of the solution (mL)
W — Weight of dried resin (g)
ΔG — Standard Gibbs free energy change (kJ·mol^{-1})
ΔH — Enthalpy of reaction (kJ·mol^{-1})
ΔS — Entropy of reaction (J·mol^{-1}·K^{-1})
a_E — Initial sorption rate of the Elovich equation
b_E — Desorption constantf the Elovich equation
β — D-R isotherm constant (mol^2·J^{-2})
ε — Polanyi potential (J·mol^{-1})

References

[1] M.H. Morcali, B. Zeytuncu, A. Baysal, S. Akman, O. Yucel, Adsorption of copper and zinc from sulfate media on a commercial sorbent, J. Environ. Chem. Eng., 2 (2014) 1655–1662.

[2] H. Serencama, D. Ozdesb, C. Duranc, H.B. Senturk, Assessment of kinetics, thermodynamics, and equilibrium parameters of Cu(II) adsorption onto Rosa canina seeds, Desal. Water Treat., 52 (2014) 3226–3236.

[3] S. Rengaraj, Y. Kim, C.K. Joo, K. Choi, J. Yi, Batch adsorptive removal of copper ions in aqueous solutions by ion exchange resins: 1200H and IRN97H, Korean J. Chem. Eng., 21 (2004) 187–194.

[4] M. Ajmal, R.A.K. Rao, M. A. Khan, Adsorption of copper from aqueous solution on *Brassica cumpestris* (mustard oil cake), J. Hazard. Mater. B, 122 (2005) 177–183.

[5] J.R. Njimou, A. Măicăneanu, C. Indolean, C.P. Nanseu-Njiki, E. Ngameni, Removal of Cd (II) from synthetic wastewater by alginate–Ayous wood sawdust (Triplochiton scleroxylon) composite material, Environ. Technol., 37 (2016) 1369–1381.

[6] L.X. Zhong, X.W. Peng, L.X. Song, D. Yang, X.F. Cao, R.C. Sun, Adsorption of Cu^{2+} and Ni^{2+} from aqueous solution by arabinoxylan hydrogel: equilibrium, kinetic, competitive adsorption, Separ. Sci. Technol., 48 (2013) 2659–2669.

[7] S. Yin, C.H. Feng, Y.Y. Li, L.F. Yin, Z.Y. Shen, Heavy metal pollution in the surface water of the Yangtze Estuary: A 5-year follow-up study, Chemosphere, 138 (2015) 718–725.

[8] B. Alyüz, S. Veli, Kinetics and equilibrium studies for the removal of nickel and zinc from aqueous solutions by ion exchange resins, J. Hazard. Mater., 167 (2009) 482–488.

[9] P.E. Franco, M.T. Veit, C.E. Borba, G.C. Gonçalves, M.R. Fagundes-Klen, R. Bergamasco, E.A. Silva, P.Y.R. Suzaki, Nickel(II) and zinc(II) removal using Amberlite IR-120 resin: Ion exchange equilibrium and kinetics, Chem. Eng. J., 221 (2013) 426–435.

[10] A.E. Hamidi, R.M. Masamba, M. Khachani, M. Halim, S. Arsalane, Kinetics modeling in liquid phase sorption of copper ions on brushite di-calcium phosphate di-hydrate $CaHPO_4·2H_2O$ (DCPD), Desal. Water Treat., 56 (2015) 779–791.

[11] B.A. Fil, R.B. Boncukcuoglu, A.E. Yilmaz, S. Bayar, Adsorption of Ni(II) on ion exchange resin: kinetic, equilibrium and thermodynamic studies, Korean J. Chem. Eng., 29 (2012) 1232–1238.

[12] S. Rengaraj, J.W. Yeon, Y. Kim, Y. Jung, Y.K. Ha, W.H. Kim, Adsorption characteristics of Cu(II) onto ion exchange resins 252H and 1500H: kinetics, isotherms and error analysis, J. Hazard. Mater., 143 (2007) 469–477.

[13] L.C. Lin, R.S. Juang, Ion-exchange equilibria of Cu(II) and Zn(II) from aqueous solutions with Chelex 100 and Amberlite IRC 748 resins, Chem. Eng. J., 112 (2005) 211–218.

[14] T.N. Kwon, C. Jeon, Adsorption characteristics of sericite for nickel ions from industrial waste water, J. Ind. Eng. Chem., 19 (2013) 68–72.

[15] M.K. Jha, N.V. Nguyen, J.C. Lee, L. Jeong, J.M. Yoo, Adsorption of copper from the sulphate solution of low copper contents using the cationic resin Amberlite IR 120, J. Hazard. Mater., 164 (2009) 948–953.

[16] I. Langmuir, The adsorption of gases on plane surfaces of glass, mica and platinum, J. Am. Chem. Soc., 40 (1918) 1361–1403.

[17] K.R. Hall, L.C. Eagleton, A. Acrivos, T. Vermeulen, Pore-and solid-diffusion kinetics in fixed-bed adsorption under constant-pattern conditions, Ind. Eng. Chem. Fundam., 5 (1966) 212–223.

[18] H.M.F. Freundlich, Over the adsorption in solution, J. Phys. Chem., 57 (1906) 385–470.

[19] M.J. Temkin, V. Pyzhev, Recent modifications to Langmuir isotherms, Acta Physiochim. USSR, 12 (1940) 217–222.

[20] R.J. Qu, C.M. Sun, F. Ma, Z.Z. Cui, Y. Zhang, X.Y. Sun, C.N. Ji, C.H. Wang, P. Yin, Adsorption kinetics and equilibrium

of copper from ethanol fuel on silica-gel functionalized with amino-terminated dendrimer-like polyamidoamine polymers, Fuel, 92 (2012) 204–210.

[21] M.M. Dubinin, E.D. Zaverina, L.V. Radushkevich, Sorption and structure of active carbons. I. Adsorption of organic vapors, Zh. Fiz. Khim., 21 (1947) 1351–1362.

[22] I. Kiran, T. Akar, A.S. Ozcan, A. Ozcan, S. Tunali, Biosorption kinetics and isotherm studies of Acid Red 57 by dried Cephalosporium aphidicola cells from aqueous solutions, Biochem. Eng. J., 31 (2006) 197–203.

[23] R. Donat, A. Akdogan, E. Erdem, H. Cetisli, Thermodynamics of Pb^{2+} and Ni^{2+} adsorption onto natural bentonite from aqueous solutions, J. Colloid Interf. Sci., 286 (2005) 43–52.

[24] S. Lagergren, About the theory of so called adsorption of soluble substances, Kungliga Svenska Vetenskapsakademiens, Handlingar Band, 24 (1898) 1–39.

[25] Y.S. Ho, G. McKay, Pseudo-second order model for sorption processes, Proc. Biochem., 34 (1999) 451–465.

[26] J.S. Cao, J.X. Lin, F. Fang, M.T. Zhang, Z.R. Hu, A new absorbent by modifying walnut shell for the removal of anionic dye: Kinetic and thermodynamic studies, Bioresour. Technol., 163 (2014) 199–205.

[27] Z.P. Gao, Z.F. Yu, T.L. Yue, S.Y. Quek, Adsorption isotherm, thermodynamics and kinetics studies of polyphenols separation from kiwifruit juice using adsorbent resin, J. Food Eng., 116 (2013) 195–201.

[28] P.S. Kumar, C. Senthamarai, A. Durgadevi, Adsorption kinetics, mechanism, isotherm, and thermodynamic analysis of copper ions onto the surface modified agricultural waste, Environ. Prog. Sustain. Energy, 33 (2014) 28–37.

[29] T.Y. Kim, S.S. An, W.G. Shim, J.W. Lee, S.Y. Cho, J.H. Kim, Adsorption and energetic heterogeneity properties of cesium ions on ion exchange resin, J. Ind. Eng. Chem., 27 (2015) 260–267.

[30] Z.H. Yu, T. Qi, J.K. Qu, L.N. Wang, J.L. Chu, Removal of Ca(II) and Mg(II) from potassium chromate solution on Amberlite IRC 748 synthetic resin by ion exchange, J. Hazard. Mater., 167 (2009) 406–412.

[31] R. Laus, V.T. de Fávere, Competitive adsorption of Cu(II) and Cd(II) ions by chitosan crosslinked with epichlorohydrin-triphosphate, Bioresour. Technol., 102 (2011) 8769–8776.

[32] H. Leinonen, J. Lehto, Ion-exchange of nickel by iminodiacetic acid chelating resin Chelex 100, React. Funct. Polym., 43 (2000) 1–6.

[33] F. Gode, E. Pehlivan, Removal of chromium(III) from aqueous solutions using Lewatit S 100: the effect of pH, time, metal concentration and temperature, J. Hazard. Mater., B136 (2006) 330–337.

[34] J.B. Yang, M.Q. Yu, T. Qiu, Adsorption thermodynamics and kinetics of Cr(VI) on KIP210 resin, J. Ind. Eng. Chem., 20 (2014) 480–486.

[35] E. Pehlivan, T. Altun, The study of various parameters affecting the ion exchange of Cu^{2+}, Zn^{2+}, Ni^{2+}, Cd^{2+}, and Pb^{2+} from aqueous solution on Dowex 50W synthetic resin, J. Hazard. Mater., B134 (2006) 149–156.

[36] A. Sari, D. Mendil, M. Tuzen, M. Soylak, Biosorption of Cd(II) and Cr(III) from aqueous solution by moss (Hylocomium splendens) biomass: Equilibrium, kinetic and thermodynamic studies, Chem. Eng. J., 144 (2008) 1–9.

[37] W.X. Zhang, H.J. Li, X.W. Kan, L. Dong, H. Yan, Z.W. Jiang, H. Yang, A.M. Li, R.S. Cheng, Adsorption of anionic dyes from aqueous solutions using chemically modified straw, Bioresour. Technol., 117 (2012) 40–47.

[38] V.C. Srivastava, M.M. Swamy, I.D. Mall, B. Prasad, I.M. Mishra, Adsorptive removal of phenol by bagasse fly ash and activated carbon: Equilibrium, kinetics and thermodynamics, Colloid. Surface. A, 272 (2006) 89–104.

[39] W. Kossel, Molecular formation as an issue of the atomic construction, Ann. Phys., 49 (1916) 229–362.

[40] L. Paulling, The principles determining the structure of complex ionic crystals, J. Am. Chem. Soc., 51 (1929) 1010–1026.

[41] Z.A. AL-Othman, Mu. Naushad, A. Nilchi, Development, characterization and ion exchange thermodynamics for a new crystalline composite cation exchange material: application for the removal of Pb^{2+} ion from a standard sample (Rompin Hematite), J. Inorg. Org. Polym. Mater., 21 (2011) 547–559.

[42] M. Naushad, Surfactant assisted nano-composite cation exchanger: Development, characterization and applications for the removal of toxic Pb^{2+} from aqueous medium, Chem. Eng. J., 235 (2014) 100–108.

[43] L. Meites, E. McGraw-Hill, Handbook of Analytical Chemistry, New York, 1963.

[44] A. Agrawal, K.K. Sahu, J.P. Rawat, Kinetic studies on the exchange of bivalent metal ions on Amberlite IRC-718 - An Iminodiacetate resin, Solvent Extr. Ion Exc., 21 (2003) 763–782.

[45] Z.X. Zeng, L. Cui, W.L. Xue, N.K. Ma, Study on adsorption behavior of 12-Phosphotungstic acid on Silica gel, Ind. Eng. Chem. Res., 52 (2013) 8070–8078.

[46] H.Y. Ye, J. Pi, Z.H. Li, Q.R. Yang, J.Y. Cai, Investigation on the structures of hydrated metal ion clusters, Sci. Technol. Dev., S1 (2010) 182–184. (in Chinese)

[47] K. Ebitani, K. Nagashima, T. Mizugaki, K. Kaneda, Preparation of a zeolite X-encapsulated copper(II) chloride complex and its catalysis for liquid-phase oxygenation of enamines in the presence of molecular oxygen, Chem. Commun., (2000) 869–870.

[48] T. Kawabata, M. Kato, T. Mizugaki, K. Ebitani, K. Kaneda, Monomeric metal aqua complexes in the interlayer space of montmorillonites as strong lewis acid catalysts for heterogeneous carbon–carbon bond-forming reactions, Chem. Eur. J., 11 (2005) 288-297.

[49] A.J. Stace, N.R. Walker, S. Firth, $[Cu(H_2O)_n]^{2+}$ clusters: the first evidence of aqueous Cu(II) in the gas phase, J. Am. Chem. Soc., 119 (1997) 10239–10240.

[50] H.Y. Liu, C.H. Fang, Y. Fang, Y.Q. Zhou, H.W. Ge, F.Y. Zhu, P.C. Sun, J.T. Miao, Characterizing Ni(II) hydration in aqueous solution using DFT and EXAFS, J. Mol. Model., 22 (2016) 1–9.

[51] F.F. Xia, D.W. Zeng, H.B. Yi, C.H. Fang, Direct contact vs. solvent-shared ion pairs in saturated $NiCl_2$ aqueous solution: A DFT, CPMD, and EXAFS investigation, J. Phys. Chem. A, 117 (2013) 8468–8476.

[52] Y.G. Liu, Fundamental elements chemistry, Beijing, 1992. (in Chinese)

[53] H. Matsumiya, M. Kuromiya, M. Hiraide, Matrix-precipitation for the determination of trace impurities in high-purity Iron, ISIJ International, 53 (2013) 81–85.